

# PyraTrans: Learning Attention-Enriched Multi-Scale Pyramid Network from Pre-Trained Transformers for Effective Malicious URL Detection

Ruitong Liu, Yanbin Wang\*, Zhenhao Guo, Haitao Xu<sup>✉</sup>, Zhan Qin, Wenrui Ma, Fan Zhang

**Abstract**—Detecting malicious URLs is a crucial aspect of web search and mining, significantly impacting internet security. Though advancements in machine learning have improved the effectiveness of detection methods, these methods still face significant challenges in their capacity to generalize and their resilience against evolving threats. In this paper, we propose PyraTrans, an approach that combines the strengths of pretrained Transformers and pyramid feature learning for improving malicious URL detection. We implement PyraTrans by leveraging a pretrained CharBERT as the base and augmenting it with 3 connected feature modules: 1) The Encoder Feature Extraction module, which extracts representations from each encoder layer of CharBERT to obtain multi-order features; 2) The Multi-Scale Feature Learning Module, which captures multi-scale local contextual insights and aggregate information across different layer-levels; and 3) The Pyramid Spatial Attention Module, which learns hierarchical and spatial feature attentions, highlighting critical classification signals while reducing noise. The proposed approach addresses the limitations of the Transformer in local feature learning and spatial awareness, and enabling us to extract multi-order, multi-scale URL feature representations with enhanced attentional focus. PyraTrans is evaluated using 4 benchmark datasets, where it demonstrated significant advancements over prior baseline methods. Particularly, on the imbalanced dataset, our method, trained with 60% of the data, achieves a TPR increase of 16-24 points and an F1-score improvement of 12-27 points. With just 10% of the data for training, the TPR is 3.3-6.5 times and the F1-score is 2.9-4.5 times that of the baseline. Additionally, our approach not only demonstrates robustness against adversarial sample attacks, achieving an accuracy of 0.9023, significantly surpassing the best baseline accuracy of 0.7610, but it shows improved generalization in cross-dataset evaluation experiments. We also executed case studies on 30 active malicious websites, where our technique achieved 100% accuracy in identifying all malicious sites. Codes and data are available at: <https://github.com/Alixyvtte/PyraTrans>.

**Index Terms**—Cybersecurity, Phishing Detection, Transformer, Pre-trained Language Model, Deep Learning

## I. INTRODUCTION

**M**ALICIOUS URLs, systematically engineered by cybercriminals for illicit activities such as scams, phishing, spam, and malware distribution, constitute a significant cybersecurity risk. These URLs directly threaten user and organizational security, leading to privacy breaches, data theft, extortion, and compromising the integrity of devices and networks. Vade's 2023-Q3 report highlights a substantial escalation in phishing and malware incidents. The period saw malware volumes nearing the highest quarterly record, second only to Q4 2016's 126.8 million instances. A notable 173% increase in phishing incidents was reported over the previous

quarter, totaling 493.2 million, the highest for any Q3 since systematic tracking began in 2015 [1].

Predominantly, cyber attackers leverage deceptive hyperlinking as a key strategy in phishing schemes, often imitating credible entities like Microsoft, Google, and Facebook [2]. The ability to alter the display text of hyperlinks in HTML exacerbates the threat by camouflaging the true malicious nature of these URLs. This tactic poses a significant challenge to the detection of malicious URLs. Traditional database-centric detection platforms, such as Phishtank, reliant on community submissions, often face delays in identifying and mitigating new threats. The urgency for advanced systems capable of adapting to the dynamic cybersecurity environment and effectively identifying deceptive malicious URLs is highlighted by this lag.

Traditional methods for detecting malicious URLs, such as blacklist, heuristic, and rule-based approaches, face limitations as they require a understanding of URL structures and nature (as depicted in Figure 1 [3], [4]. Blacklist detection encounters issues such as delayed updates and struggles with identifying unknown malicious URLs. Heuristic methods show performance variations across different malicious URL samples, while rule-based detection needs manual maintenance, making it challenging to address emerging threats and their variations [5], [6]. These limitations highlight the need for utilizing more advanced machine learning methods. On the other hand, earlier studies illustrates that malicious URLs display highly discernible string patterns, including length, the quantity of dots, and specific words [7], [8]. These patterns play a vital role in threat analysis and provide the groundwork for training sophisticated classifiers.

Advancements in deep learning have significantly propelled the development of malicious URL detection systems [9]. Utilizing stacked nonlinear layers, deep learning [10], [11] learns to extract abstract, dense representations from raw initial feature vectors, such as character-level, word-level, or n-gram-based features, circumventing the need for intricate expert feature engineering. Convolutional Neural Networks (CNNs) have been the predominant deep learning models in prior malicious URL detection efforts like URLNet [12], TException [13], and Grambeddings [14], where CNNs capture local URL patterns to achieve SOTA performance. However, the technical limitations of CNNs make it increasingly difficult to achieve significant improvements in the development of CNN-based malicious URL detection models.

Recently, pretrained Transformer frameworks, such as

TABLE I  
EXAMPLE OF THE BERT TOKEN SEQUENCE EXTRACTION FROM AMAZON WEB PAGE.

URL	<a href="https://www.contactmailsupport.net/customer-service/amazon/">https://www.contactmailsupport.net/customer-service/amazon/</a>
Token Sequence	'[CLS]', 'https', ':', '/', '/', 'www', '/', 'contact', '#mail', '#su', '#pp', '#ort', '.', 'net', '/', 'customer', '−', 'service', '/', 'am', '#az', '#on', '/', '[SEP]'



Fig. 1. Some major parts in a URL.

BERT [15], have demonstrated promising prospects in various fields including natural language understanding, computer vision, and bioinformatics. This novel computational architecture and training paradigm offer new opportunities in malicious URL detection [16], [17]. They not only have stronger contextual learning capabilities but are also purely data-driven, end-to-end models. Table I presents an example of a BERT token sequence generated from a URL. However, despite the success of pretrained Transformer across multiple disciplines, their technological advantages have yet to be fully explored and manifested in malicious URL detection.

In this study, we propose PyraTrans, a novel approach developed on the foundation of pretrained Transformers, aimed at effectively detecting malicious URLs. This method exploits the various encoding layers of pre-trained Transformers and amalgamates them with multi-scale feature extraction and pyramid attention. Our approach, when tested across a broad range of public benchmarks datasets, exhibited superior performance over previous methods, proving to be more generalizable and robust, particularly in challenging situations like adversarial sample attacks, cross-dataset evaluation, class-imbalanced learning. We also conduct a case study to evaluate the model in real-world applications.

The main contributions of this paper are as follows:

- Our method establishes new state-of-the-art performance in malicious URL detection, achieving over a 10% performance increase across various test scenarios compared to current state-of-the-art methods. In certain challenging scenarios, the improvement in the F1-score even reaches 40 points.
- Our approach leverages the multi-layer encoding capability of Transformers to construct a multi-order URL representation. Through empirical analysis, we have found that this layered Transformer encoding significantly improves performance in detecting malicious URLs.
- By embedding multi-scale feature learning and pyramid attention into the pre-trained Transformer architecture, our method rectifies the inherent limitations of Transformers in terms of local feature extraction and spatial relationship perception.
- Our research exposes weaknesses in generalization and robustness in previous methods. Particularly, our case

study demonstrates a significant decrease in the detection success rate of these methods when applied in practical applications. In contrast, our approach has improved performance in these critical aspects.

The paper unfolds as follows: Section II conducts a literature review, while Section III outlines the datasets used. In Section IV, we provide a thorough explanation of the architecture and key components within our model. V details extensive experiments on malicious URL detection, benchmarking against baseline methods. A case study is then provided in Section V-E, and our conclusions are summarized in Section VII.

## II. RELATED WORK

Malicious URL detection has a long-standing history in research. In this paper, we primarily review some recent works relevant to our study, which can be categorized into two types: CNN-based approaches and Transformer-based approaches.

### A. CNN-based Detection

Huang et al. [18] proposed a network that incorporates convolutional layers and two capsule network layers to learn the embedding representations of URLs. Wang et al. [19] combined CNNs and RNNs to extract key features for measuring content similarity, integrating these with static lexical features extracted from URLs using Word2Vec for their detection model. URLNet [12] introduced a dual-channel CNN approach for learning both character and word-level embeddings, combining these at the model's top. This method not only achieved state-of-the-art performance at the time but also inspired numerous subsequent studies [13], [20]–[22], which all adopted the dual-channel feature extraction concept of URLNet. Recently, Bozkir et al. [14] developed Grambeddings, a neural network that effectively combines CNNs, LSTMs, and attention mechanisms. This network represents URL features through n-grams and has shown performance that surpasses URLNet in certain aspects.

The application of traditional neural networks in this field has seen widespread adoption. However, recent research suggests that their performance appears to have reached a plateau, leaving limited room for further improvement. Moreover, although these methods have advanced malicious URL detection, they still rely on manually initialized features at different levels (characters, words, or n-grams). In contrast, our proposed method is purely data-driven, requiring no manual engineering, and ingeniously implements feature extraction at both subword and character levels.

TABLE II  
THE STATISTICAL ANALYSIS OF OUR DATASETS

Dataset	Sample Sizes			Avg Length		Benign TLDs			Malicious TLDs		
	malicious <sup>5</sup>	benign	total	malicious	benign	.com	ccTLDs	others	.com	ccTLDs	others
GramBeddings <sup>1</sup>	400,000	400,000	800,000	86.24	46.38	52.17%	12.04%	35.79%	60.10%	11.82%	28.08%
Mendeley <sup>2</sup>	35,315	1,526,619	1,561,934	37.15	35.82	61.97%	0.93%	37.10%	72.86%	1.61%	25.53%
Kaggle 1 <sup>3</sup>	316,251	316,252	632,503	64.68	58.30	77.46%	0.63%	21.92%	50.59%	10.61%	38.8%
Kaggle 2 <sup>4</sup>	213,037	428,079	641,116	64.13	57.69	74.27%	6.61%	19.12%	46.62%	7.74%	45.65%

<sup>1,2</sup> These are used for binary classification, download using Grambeddings and Mendeley links.

<sup>3</sup> This is used for binary cross dataset test, download using this link.

<sup>4</sup> This is used for multiple classification, download using this link.

<sup>5</sup> Indicates malicious URLs in binary test and the total of malicious, defacement, and phishing URLs in multiple test.

### B. Transformer-based Detection

Chang et al. [11] fine-tuned a BERT model, initially pre-trained on English text, using URL data for detecting malicious URLs. URLTran [10] comprehensively analyzed transformer models for phishing URL detection, demonstrating their feasibility and exploring various hyperparameter settings. However, these approaches, due to limited technical modifications, could not overcome the bias between the pretrained data domain and the task domain. The study in [23] employed a Transformer with a hybrid expert network for URL classification. Xu et al. [24] used a lightweight Transformer-based model. Although these methods achieved good performance, they did not fully leverage the advantages of pretraining. In the work of Wang et al. [25], a domain-specific BERT architecture was pretrained from scratch for URL applications. While this approach offers many benefits, it requires extensive URL data, substantial computational resources, and extensive training time.

### III. LARGE SCALE URL DATASET

The four datasets used for training, validation and testing are publicly available. These datasets share a similar schema, consisting of the browsing URL and a corresponding label indicating whether the URL has been identified as malicious or benign. Upon analyzing their statistical data, including sample size, average URL length, and top-level domain (TLD) types, as shown in TableII, we discovered certain variations in the URL data across these datasets, which contribute to a more comprehensive evaluation of our model.

**GramBeddings Dataset:** As provided by Grambeddings [14], this dataset comprises 800,000 samples, equally divided into 400,000 malicious and 400,000 benign URLs. Malicious URLs were collected from websites such as PhishTank and OpenPhish, spanning the period from May 2019 to June 2021. Long-Term and Periodical Sampling, as well as Similarity Reduction techniques, were applied to the malicious data. The benign URLs were iteratively crawled from Alexa and the top 20 most popular websites in 20 different countries, and then randomly sampled. As a result, this dataset presents the highest diversity and sample size compared to others, while also demonstrating an equal number of instances per class. As shown in the table, the average length of malicious URLs is significantly longer than that of benign URLs, approaching twice the length, ensuring the similarity of the class-level average length distribution. In terms of top-level domain

(TLD) features, because different domains are generally more difficult to obtain in malicious URLs, this dataset has improved the domain-level diversity of malicious URLs by setting a low ratio of unique domains to total domains, achieving a ratio similar to that of benign URLs, with *.com* at 60.10% and ccTLDs at 11.82%, whereas for benign URLs, it is *.com* at 52.17% and ccTLDs at 12.04%.

**Mendeley Dataset:** From Mendeley Data [26], this dataset consists of 1,561,934 samples, with a significant skew towards benign URLs (1,526,619) compared to 35,315 malicious URLs. The samples were crawled using the MalCrawler tool and validated using the Google Safe Browsing API [27]. This dataset exhibits a notable class imbalance at a ratio of approximately 1:43. In terms of average length, both malicious and benign URLs demonstrate similar values, and the diversity of top-level domains (TLDs) is limited, primarily concentrated in *.com*, accounting for 61.97% and 72.86%, respectively, with ccTLDs representing only 0.93% and 1.61%. Although this may pose a risk of misleading the training processes by capturing inadequate syntactical or semantic features, considering the potential encounter with such data distribution in real-world scenarios, we chose to employ this dataset for model evaluation.

**Kaggle Dataset:** The Kaggle 1 and Kaggle 2 datasets are both derived from the Kaggle website. Kaggle 1 is designed for binary classification experiments, while Kaggle 2 is intended for multi-classification tasks. Kaggle 1 consists of 632,503 samples, evenly distributed between malicious and benign URLs. In comparison to the Mendeley dataset, this dataset demonstrates disparity in the average length of malicious and benign URLs, with the samples presenting a more balanced composition between the two classes. Notably, within the malicious samples of this dataset, there is a noticeable higher ratio of ccTLDs in TLDs compared to the benign URLs, accounting for 10.61%, while benign URLs only make up 0.63%. Additionally, the proportion of *.com* domains is 50.59% for malicious URLs, whereas it is 77.46% for benign URLs.

The Kaggle 2 dataset consists of four classes: benign (428,079), defacement (95,306), phishing (94,086), and malicious (23,645). The benign class contains positive samples, while the other three classes contain negative samples of different types. We observe that the *.com* TLDs are dominant in benign URLs, accounting for 74.27% of the total. The ccTLDs are slightly more frequent in this dataset (6.61%) than

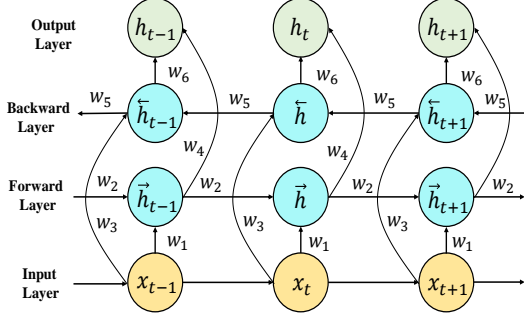


Fig. 2. The architectural diagram of BiGRU.

in the other two datasets, while the other gTLDs represent 19.12% of the benign URLs. For the negative samples, the .com TLDs are less prevalent, with a frequency of 46.62% across all three classes. The ccTLDs and other gTLDs have higher frequencies of 7.74% and 45.65%, respectively, in the negative samples than in the benign ones.

The distinctive composition and Top-Level Domain (TLD) distribution in each dataset offer a comprehensive foundation for assessing the efficacy of our method across diverse web domains. This enables robust testing under different real-world scenarios.

#### IV. METHODOLOGY

We propose a method that incorporates a backbone network constructed by the CharBERT model, along with three feature modules: the Encoder Feature Extraction module, the Multi-scale Learning module, and the Pyramid Spatial Attention module.

The overall model structure is depicted in Fig. 3.

- **Backbone Network:** The CharBERT model, acting as the backbone network, improves URL data interpretation and analysis with its advanced subword and character-level embedding which extends based on BERT.
- **Encoder Feature Extraction:** This module aggregates and extracts multi-level features, employing a novel feature integration approach to effectively capture and utilize both high-level and low-level features from encoders.
- **Multi-scale Learning:** This module is designed to capture features of different scales and granularities and extract both local and global features from URL strings. While maintaining a lightweight structure, it adaptively recalibrates the information flow from multiple channels, enhancing the model's focus on key data aspects.
- **Pyramid Spatial Attention:** This module emphasizes the contextual relevance of various layers within the network. It enhances the base network by laterally incorporating Spatial Pyramid Attention (SPA) Blocks, prioritizing specific features over others based on their contextual importance.

##### A. Backbone Network

We employ the pretrained CharBERT [28] as our backbone network, chosen for its simultaneous focus on subword and

character-level features of text. CharBERT, an extension of the BERT model, integrates the Transformer architecture with a novel dual-channel framework designed to capture information at both subword and character levels. CharBERT achieves notable progress through the implementation of two key components: (1) the Character Embedding Module, encoding character sequences from input tokens and (2) the Heterogeneous Interaction Module, combines features from both character and subword channels, and then independently separates them into distinct representations as input for the encoder layer.

Within the character embedding module, we generate token-level embeddings by incorporating character-level information into input sentences. The character-aware embedding of each token is primarily generated through two components: the encoding of individual characters and subword units. These two components are integrated via a dual-channel architecture. To establish contextual character embeddings, we utilize a bidirectional Gated Recurrent Unit (BiGRU) layer. The BiGRU employs a bidirectional recurrent neural network with only the input and forget gates [29]. The architecture diagram of the BiGRU is depicted in Figure 2.

Assuming  $x$  denotes the input data, and  $h$  represents the output of GRU unit.  $r$  is the reset gate, and  $z$  is the update gate.  $r$  and  $z$  decide how to get the new hidden state  $h_t$  from the previous hidden state  $h_{t-1}$  calculation. The update gate controls both the current input  $x_t$  and the previous memory  $h_{t-1}$ , and outputs a numerical value  $z_t$  between 0 and 1. The calculation formula is as follows:

$$z_t = \sigma(W_z[h_{t-1}, x_t] + b_z) \quad (1)$$

where  $z_t$  determines the extent to which  $h_{t-1}$  should influence the next state,  $\sigma$  is the sigmoid activation function,  $W_z$  is the update gate weight, and  $b_z$  is the bias. The reset gate regulates the influence of the previous memory  $h_{t-1}$  on the current memory  $h_t$ , removing it if deemed irrelevant.

$$r_t = \sigma(W_r[h_{t-1}, x_t] + b_r) \quad (2)$$

Then creating new memory information  $h_t$  using the update gate:

$$\tilde{h}_t = \tanh(W_h[r_t h_{t-1}, x_t] + b_h) \quad (3)$$

The output at the current moment can be obtained:

$$h_t = (1 - z_t)h_{t-1} + z_t \tilde{h}_t \quad (4)$$

The current hidden layer state of the BiGRU is influenced by the current input  $x_t$ , the forward hidden state  $h_{t-1}$ , and the output  $\tilde{h}_t$  of the reverse hidden layer state:

$$\stackrel{\rightarrow}{h_t} = \stackrel{\longrightarrow}{GRU}(h_{t-1}, x_t) \quad (t = 1, 2, \dots, d) \quad (5)$$

$$\stackrel{\leftarrow}{h_t} = \stackrel{\longleftarrow}{GRU}(h_{t+1}, x_t) \quad (t = d, d-1, \dots, 1) \quad (6)$$

$$h_t = w_t \stackrel{\rightarrow}{h_t} + v_t \stackrel{\leftarrow}{h_t} + b_t = BiGRU(x_t) \quad (7)$$

The  $GRU$  represents the nonlinear transformation of the input, incorporating the degradation indicator into the associated

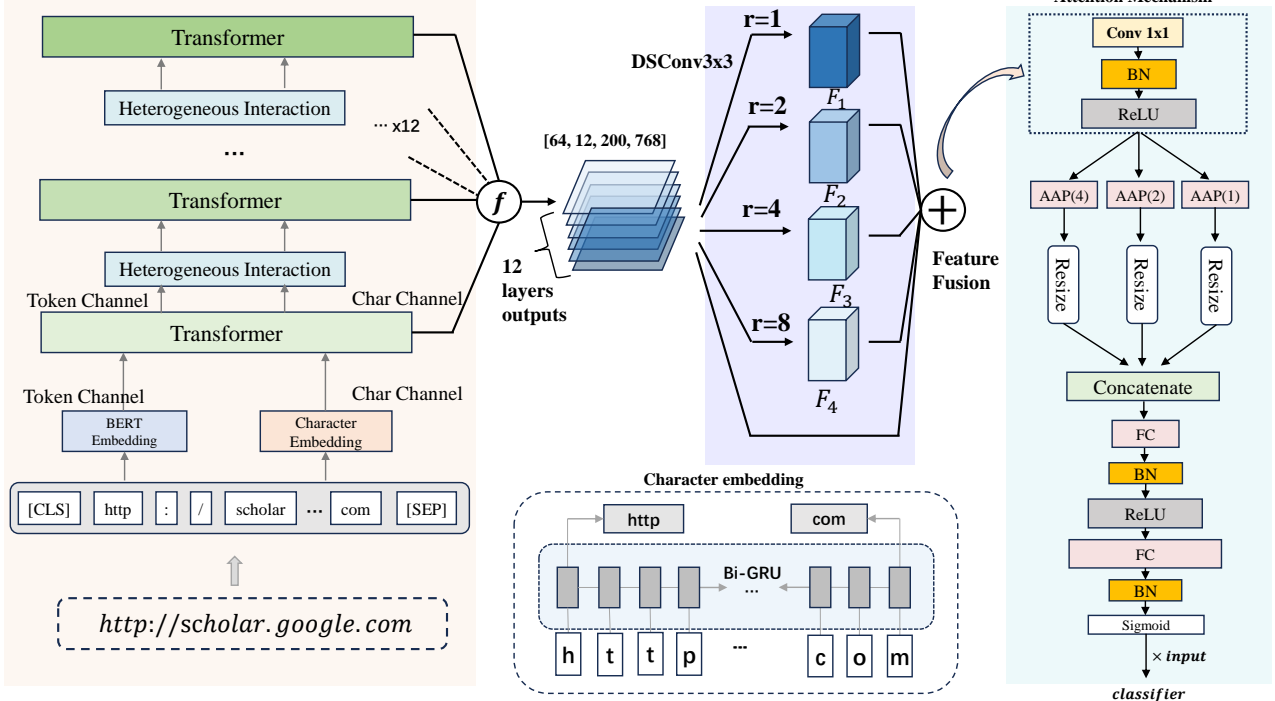


Fig. 3. PyraTrans: Consists of four essential components. CharBERT, the backbone network for feature extraction from characters and subwords; Encoder feature extraction and concatenation from different layers; A multi-scale learning module is followed by a spatial attention mechanism that adaptively reweights various informative feature channels, enhancing the classifier's ability to perform classification.

GRU hidden state.  $w_t$  and  $v_t$  denote the weights of the forward hidden layer state  $h_t$  and reverse hidden state output  $h_t$  of the bidirectional GRU at time  $t$ , respectively,  $b_t$  represents the bias corresponding to the hidden state at time  $t$ .

In the generation of character embeddings, we represent an input sequence as  $w_1, \dots, w_i, \dots, w_m$ , where  $w_i$  is a subword tokenized using Byte Pair Encoding (BPE), and  $m$  is the length of the sequence at the subword level. Each token  $w_i$  consists of characters  $c_1^i, \dots, c_{n_i}^i$ , where  $n_i$  represents the length of the subword. The total character-level input length is denoted as  $N = \sum_{i=1}^m n_i$ , where  $m$  is the number of tokens. The formulation of the processing is as follows:

$$e_j^i = W_c \cdot c_j^i; h_j^i = BiGRU(e_j^i); \quad (8)$$

Here,  $W_c$  is the character embedding matrix, and  $h_j^i$  denotes the representation of the  $j$ -th character within the  $i$ -th token. The BiGRU processes characters across the entire input sequence of length  $N$  to generate token-level embeddings. Then connect the hidden states of the first and last characters in each token, as follows:

$$h_i(x) = [h_1^i(x); h_{n_i}^i(x)] \quad (9)$$

Let  $n_i$  be the length of the  $i$ -th token, and  $h_i(x)$  be the token-level embedding from characters, enabling contextual character embeddings to capture complete word information.

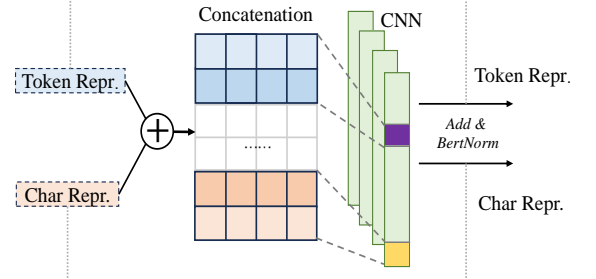


Fig. 4. The architecture of Heterogeneous Interaction Module.

The heterogeneous interaction module fuses and separates the token and character representations after each transformer layer. The structure shown in Fig4. This module uses different fully-connected layers to transform the representations, and then concatenates and integrates them by using a CNN layer, as follows:

$$t'_i(x) = W_1 * t_i(x) + b; h'_i(x) = W_2 * h_i(x) + b_2 \quad (10)$$

$$w_i(x) = [t'_i(x); h'_i(x)]; m_{j,t} = \tanh(W_{3 \times w_{t:t+s_j-1}}^j + b_j^j) \quad (11)$$

where  $t_i(x)$  is the token representation,  $W$  and  $b$  are the parameters,  $w_{t:t+s_j-1}$  is the concatenation of the embeddings of  $(w_t, \dots, w_{t+s_j-1})$ ,  $s_j$  is the window size of the  $j$ -th filter, and

TABLE III  
PERFORMANCE OF SPAN REPRESENTATION CLUSTERING DERIVED  
FROM VARIOUS LAYERS OF BERT [31]

Layer	1	2	3	4	5	6
NMI	0.38	0.37	0.35	0.3	0.24	0.2
Layer	7	8	9	10	11	12
NMI	0.19	0.16	0.17	0.18	0.16	0.19

$m$  is the fused representation, which has the same dimension as the number of filters.

Next is a fully connected layer with GELU activation [30], used to restore the fused features to two channels, with residual connection added to preserve the original information of each channel.

$$m_i^t(x) = \Delta(W_4 * m_i(x) + b_4); \quad m_i^h(x) = \Delta(W_5 * m_i(x) + b_5) \quad (12)$$

$$T_i(x) = t_i(x) + m_i^t(x); \quad H_i(x) = h_i(x) + m_i^h(x) \quad (13)$$

$\Delta$  is the activation function GELU, and  $T$  and  $H$  as the representations of the two channels. After the residual connection, a layer normalization operation is applied. The fusion and separation process can enrich the mutual representations of the two channels, while preserving the specific features of the tokens and characters. The pre-training tasks can also enhance the differentiation of the dual-channel framework.

### B. Feature Extraction

Pre-trained language models such as BERT use multiple layers of Transformer encoders to learn semantic knowledge from large-scale corpora, and then fine-tune them for specific downstream tasks. Most BERT-based classification models depend on the [CLS] feature of the final layer, which summarizes the semantic information of the whole input sequence. However, Jawahar *et al.* [31] show that BERT can learn various information across layers, such as phrase-level details in lower layers, syntactic information in middle layers, and rich semantic features in higher layers. They apply k-means clustering to the BERT layer representations and measure the cluster quality by using Normalized Mutual Information (NMI). They find that lower BERT layers are better at encoding phrase-level information, as indicated by higher NMI scores, as shown in Table III. Deeper encoder layers are more effective in handling long-range dependency information.

However, in the context of the BERT model, even though each layer of the model takes the previous layer's output features as input for computation, multiple intricate calculations within each layer's processing may still result in potential degradation of lower-level and mid-level features, which is detrimental to the complete feature learning process. Li *et al.* [32] use feature concatenation to integrate aspect features from each layer of BERT for aspect term sentiment classification. This approach, instead of relying only on the final layer for classification features, effectively enhances classification performance by leveraging the distinct features learned at each layer of BERT.

Our method uses a hierarchical feature extraction model to exploit the multi-level information from the low, middle, and high layers of CharBERT. The feature extraction process is as follows:

Consider a sequence of outputs  $k_1, k_2, \dots, k_n$  and  $u_1, u_2, \dots, u_m$ , where each output  $k_i$  and  $u_j$  has a rank of  $(H, W, C)$ , representing the outputs of CharBERT's word-level and character-level encoders at various layers.  $H$  is the batch size,  $W$  is the fixed URL sequence length (200 in our model), and  $C$  is a 768-dimensional vector for each merged hidden layer output in CharBERT. For example,  $k_1$  and  $u_2$  be two tensors representing the sequence and character embeddings, respectively. Let  $w$  be the sequence length, and  $d$  be the embedding dimension:

$$k_1 = \begin{bmatrix} x_{11}^1 & x_{12}^1 & \cdots & x_{1d}^1 \\ x_{21}^1 & x_{22}^1 & \cdots & x_{2d}^1 \\ \vdots & \vdots & \ddots & \vdots \\ x_{w1}^1 & x_{w2}^1 & \cdots & x_{wd}^1 \end{bmatrix}, \quad u_1 = \begin{bmatrix} x_{11}^2 & x_{12}^2 & \cdots & x_{1d}^2 \\ x_{21}^2 & x_{22}^2 & \cdots & x_{2d}^2 \\ \vdots & \vdots & \ddots & \vdots \\ x_{w1}^2 & x_{w2}^2 & \cdots & x_{wd}^2 \end{bmatrix} \quad (14)$$

Afterwards, we use one-dimensional convolution to fuse the concatenated channel features, reducing their dimensionality to the original values of each channel. Here,  $C$  represents concatenation,  $K_{fuse}$  denotes convolution, and  $Y$  is the resulting fused tensor:

$$Y = K_{fuse}(C(k_1, u_1)^T) = \begin{bmatrix} y_{11} & y_{21} & \cdots & y_{m1} \\ y_{12} & y_{22} & \cdots & y_{m2} \\ \vdots & \vdots & \ddots & \vdots \\ y_{1d} & y_{2d} & \cdots & y_{md} \end{bmatrix} \quad (15)$$

By stacking the merged output along the new dimension 0, we form a tensor  $F$  of rank  $(N, H, W, C)$ , where  $N$  is the number of layers (12 in our model). To align the multilevel features for subsequent analytical tasks, the tensor elements were rearranged by permuting dimensions 0 and 1. This resulted in a tensor  $F' = (H, N, W, C)$ , which served as the stacked feature input for the next multi-attention module.

### C. Multi-scale Learning

After feature concatenation, we introduce a lightweight multi-scale module for processing text embedding information across various scales. Initially, dilated convolutions with distinct dilation rates are employed to capture multi-scale information, allowing for a larger receptive field without increasing parameters. Subsequently, we utilize depthwise separable convolutions (referred to as DSConv) [33] to enhance efficiency by reducing floating-point operations and model parameters. These convolutions serve as fundamental operators for extending network depth and width. Formally, let the input feature map be denoted as  $M \in \mathbb{R}^{C \times H \times W}$ , where  $C$  is the number of channels,  $H$  is the height, and  $W$  is the width. The process begins by applying a single DSConv (conv3 x 3) to  $M$ , extracting common information denoted as  $F_0$  for each branch. Specifically:

$$F_0 = K_0(M) \quad (16)$$

$K_0$  denotes a depthwise separable conv3 x 3 operation, and dilated DSConv3x3 with different rates are applied to  $F_0$  across branches ( $K_i$  for branch  $i$ ,  $N$  branches). Contextual information from multiple scales is integrated through element-wise summation using a residual connection, termed:

$$F_i = K_i(F_0), i = 1, 2, \dots, N \quad (17)$$

$$F = \sum_{i=0}^N F_i \quad (18)$$

Since the concatenation operation substantially amplifies channel count, leading to increased computational complexity and network parameters. Thus, we opt for element-wise summation. Lastly, aggregated features are reshaped using a 1 x 1 standard convolution. Formally:

$$Q = K_{fuse}(F) + M \quad (19)$$

$K_{fuse}$  denotes the standard conv1 x 1 operation for fusing additional information at different scales. The original feature map  $M$  is integrated as a residual connection [34], aiding gradient flow and facilitating effective training. In our experiments, dilation rates of [1, 2, 4, 8] are utilized to capture contextual information at various scales.

Within the multi-scale learning module, a straightforward element-wise summation of features from various scales may inadvertently diminish the importance of informative branches while according equal significance to all scales. To mitigate this problem, we employ a spatial pyramid attention mechanism [35], which effectively assesses subfields across multiple scales and adjusts branch weights, enhancing the overall performance.

#### D. Pyramid Spatial Attention

In the multi-scale learning module, a simple element-wise summation of features from different scales may inadvertently downplay the importance of informative branches, treating all scales equally. To address this issue, we employ a spatial pyramid attention mechanism [35], which evaluates subfields across multiple scales, adjusts branch weights, and enhances overall performance.

The spatial pyramid attention mechanism comprises three key elements: point-wise convolution, spatial pyramid structure, and a multi-layer perceptron. The point-wise convolution aligns channel dimensions and consolidates channel information. The spatial pyramid structure incorporates adaptive average pooling of three different sizes, promoting structural regularization and information integration along the attention path. Multi-layer perceptron then extracts an attention map from the output of the spatial pyramid structure.

To be specific, we denoted adaptive average pooling and fully connected layer as  $P$  and  $F_{fc}$  respectively. The concatenation operation is represented as  $C$ ,  $\sigma$  denotes the Sigmoid activation function, while  $R$  is referred to as resizing a tensor to a vector. The fused feature map after the multi-scale learning module can be denoted as  $Q \in \mathbb{R}^{C \times H \times W}$ , the attention mechanism learns attention weights from the input

TABLE IV  
DETECTION RESULTS OF OUR PROPOSED METHOD VARY WITH THE NUMBER OF LAYERS EMPLOYED

# layers(count)	Accuracy	Precision	Recall	F1-score	AUC
2	0.9772	0.9811	0.9730	0.9771	0.9959
3	0.9837	0.9873	0.9799	0.9863	0.9963
4	0.9856	0.9917	0.9792	0.9854	0.9938
5	0.9860	0.9861	0.9858	0.9859	0.9998
<b>12</b>	<b>0.9915</b>	<b>0.9949</b>	<b>0.9880</b>	<b>0.9914</b>	<b>0.9965</b>

and multiplies each channel in it by learnable weights to produce an output. The output of the spatial pyramid structure  $S(Q)$  can be presented as:

$$S(Q) = C(R(P(Q, 4)), R(P(Q, 2)), R(P(R, 1))) \quad (20)$$

Omitting the batch normalization and activation layers for the sake of clarity, the fundamental transformation  $\sigma$  can be expressed as:

$$\zeta(Q) = \sigma(F_{fc}(F_{fc}(S(Q)))) \quad (21)$$

In our experiments, the channel number  $C$  is 12 according to the former process and we adopt 3-level pyramid average pooling. In the concluding phase of our network, we apply Mean Pooling to the weighted feature map along the fixed sequence length dimension. This outcome is then integrated with a dropout layer, followed by a fully connected layer that converts URL features into a binary class representation for prediction.

## V. EXPERIMENTS

This section presents the detailed experimental setup and results to assess the effectiveness of our proposed method and compare it with baselines. Our experiments are primarily divided into the following components:

- 1) Evaluation of configurations of stacked feature layers for multi-layer feature extraction.
- 2) Investigation of model data scale dependency through experiments with diverse training dataset sizes.
- 3) Varying the size of training datasets to assess the model's sensitivity to data scale.
- 4) Evaluation of multi-class classification performance.
- 5) Robustness assessment through adversarial sample testing.
- 6) Examining instances of the lastest active malicious URLs to evaluate the practicality.

**Setup.** Considering the scale of the detection task and computational resources, we opted for the pre-trained Char-BERT based on BERT. This model was trained on the English Wikipedia corpus, consisting of a total of 12GB and approximately 2,500 million words. Hyperparameter tuning during fine-tuning led to a batch size of 64, AdamW optimizer (initial learning rate: 2e-5, weight decay: 1e-4), 0.1 dropout rate, and 5 training epochs. We utilized PyTorch 2.0, NVIDIA CUDA 11.8, and Python 3.8, conducting training on NVIDIA A100

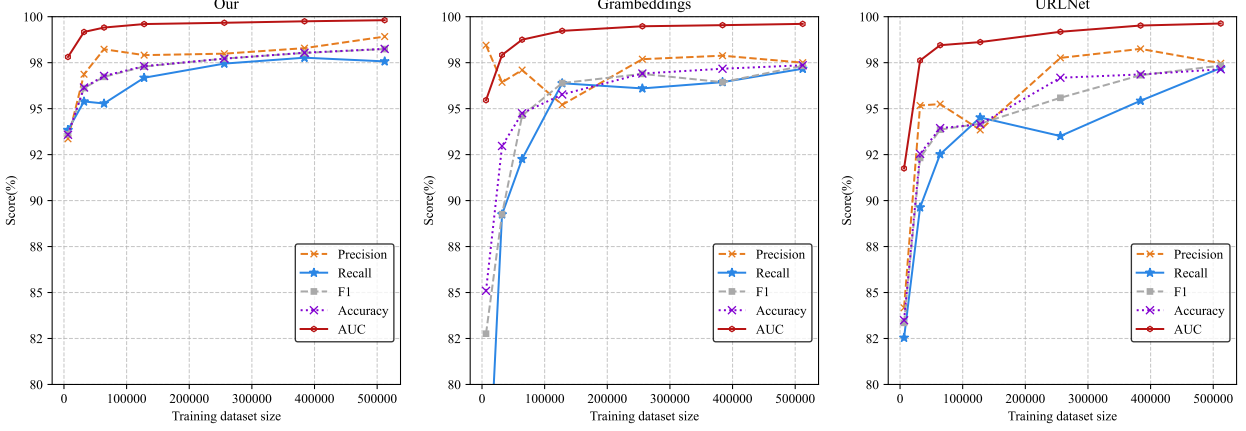


Fig. 5. Detection results of selected baseline methods and our proposed method on GramBeddings dataset.

GPUs. The final model for each experiment was selected based on the best validation loss.

**Baselines.** In our experimental comparison, we chose the state-of-the-art models, URLNet and Grambeddings, as benchmarks for evaluating our proposed method. To ensure fairness and reproducibility, we obtained their code from GitHub repositories without making any modifications to the structure or hyperparameters, and applied them to our dataset. Specifically, for URLNet, we selected Embedding Mode 5, the most complex mode, as it exhibited superior performance in their original study.

#### A. Multi-Layer Feature Evaluation

We developed a multi-layer feature extraction module to distill semantic features from different layers of the Transformer encoders in our backbone network. Our approach involves stacking embedding outputs from different layers to form a multi-layered feature matrix, which we optimized to enhance URL semantic feature representation. Through this, we investigated the complexity of feature representation across the network and aimed to demonstrate the effectiveness of multi-layered features in improving overall model performance.

We created a training corpus from the GramBeddings dataset, randomly selecting 128k URLs from the 80k available in the training set while maintaining the proportion of malicious and benign URLs. We also randomly sampled 32k URLs for testing and validation respectively. The performance of various stacked configurations and the incremental gains shown in Table IV. We observed a consistent improvement in evaluation metrics as we incrementally incorporated additional layers, namely the last 2, 3, 4, and 5 layers. Ultimately, the stacking of 12 embedding output layers achieved the best performance in URL detection tasks, demonstrating the effectiveness of integrating both lower and deeper layers in the model architecture.

#### B. Comparative Study

In this section, we compare the performance of PyraTrans with several proposed baselines using binary and multi-class

malicious URL detection datasets.

*1) Binary classification:* In the binary classification detection task, we used two datasets with significant differences. The first is the Grambeddings dataset, characterized by a balanced distribution of positive and negative samples and high diversity. The second is the Mendeley dataset, which exhibits extreme class imbalance and lower diversity. These datasets are used for evaluations in different detection scenarios. We explored the model's dependency on training data size by varying it, starting from as low as 1%. Specifically, the experimented training sizes include 1%, 5%, 10%, 20%, 40%, 60%, and 80%. And the trained models are tested across all the test datasets.

**Results on Grambeddings dataset:** As shown in Figure 5, our proposed method achieves superior performance over the baseline method on the Grambeddings dataset, regardless of the size of the training set. Remarkably, our model demonstrates high proficiency even with scarce training data.

It is worth noting that, our method achieves remarkable performance with only 6,400 URLs (1%) for training, attaining an accuracy of 0.9358, which surpasses the baseline methods that range from 0.8349 to 0.8509. Furthermore, our model exhibits a high sensitivity in detection, with a recall of 0.9384, compared to the baseline recall of 0.7131 and 0.8254. The maximum gap in F1 score reached 0.1084.

Despite the gradual improvement in the baseline model's performance with larger training samples, narrowing the gap with our method, our approach consistently achieves an accuracy of 0.9825 and an F1 score of 0.9824 using 80% of the training dataset. Our model outperformed the best baseline model with an accuracy and F1 score 0.0089 and 0.0091 higher. Although the difference seems small, it becomes significant when dealing with large-scale datasets. In conclusion, our model exhibits superior performance in accurately detecting malicious URLs on a balanced dataset, even with a small training set size.

**Results on Mendeley dataset:** To evaluate our method in real-world internet scenarios, where phishing sites are significantly outnumbered by legitimate web pages, we use

TABLE V  
DETECTION RESULTS OF SELECTED BASELINE METHODS AND OUR PROPOSED METHOD ON MENDELEY DATASET.

Training Size	Method	Accuracy	Precision	Recall	F1-score	AUC
629,184 (60%)	URLNet	0.9858	0.9475	0.3889	0.5515	0.9046
	GramBeddings	0.9801	0.6137	0.3026	0.4053	0.8205
	<b>Our</b>	0.9886	0.9104	<b>0.5419</b>	<b>0.6794</b>	<b>0.9438</b>
419,456 (40%)	URLNet	0.9842	0.9810	0.3019	0.4617	0.8992
	GramBeddings	0.9794	0.9984	0.0817	0.1510	0.8750
	<b>Our</b>	0.9882	0.8998	<b>0.5307</b>	<b>0.6677</b>	<b>0.9370</b>
209,064 (20%)	URLNet	0.9785	0.9653	0.0450	0.0860	0.7762
	GramBeddings	0.9804	0.9677	0.1306	0.2301	0.7869
	<b>Our</b>	0.9879	0.9131	<b>0.5055</b>	<b>0.6507</b>	<b>0.9322</b>
104,832 (10%)	URLNet	0.9789	0.8382	0.0735	0.1351	0.7584
	GramBeddings	0.9757	0.3879	0.1423	0.2082	0.8153
	<b>Our</b>	0.9865	<b>0.8540</b>	<b>0.4774</b>	<b>0.6125</b>	<b>0.9161</b>
104,832 (5%)	URLNet	0.9776	0.0000	0.0000	0.0000	0.6746
	GramBeddings	0.9782	0.5647	0.1139	0.1896	0.7752
	<b>Our</b>	0.9861	<b>0.8706</b>	<b>0.4397</b>	<b>0.5843</b>	<b>0.8994</b>
10,432 (1%)	URLNet	0.9776	0.0000	0.0000	0.0000	0.4419
	GramBeddings	0.9722	0.1808	0.0682	0.0991	0.6185
	<b>Our</b>	0.9834	<b>0.7632</b>	<b>0.3717</b>	<b>0.5000</b>	<b>0.8550</b>

TABLE VI  
CROSS-DATASET PERFORMANCE GENERALIZATION

Cross-dataset	Method	Accuracy	Precision	Recall	F1-score	AUC
Gram/Kaggle	URLNet	0.8823	0.8947	0.8666	0.8804	0.9492
	Grambeddings	0.5214	0.5120	0.8595	0.6552	0.4647
	<b>Our</b>	<b>0.9138</b>	<b>0.9576</b>	<b>0.8641</b>	<b>0.9085</b>	<b>0.9705</b>

the Mendeley dataset for further testing. This dataset contains 1,561,934 URLs, with a high imbalance ratio of about 43 to 1 between benign and malicious samples. This extreme imbalance poses a notable challenge to model performance, as it may cause a bias towards the abundant benign URL samples and increase the false positive rate when detecting malicious samples.

As shown in Table V, our method outperforms other methods across several metrics in a class-imbalanced scenario. Even with only 1% of training data, our model attains a 0.5 F1 score, which is four times higher than the baseline's performance. With more training data, our F1 score reaches 0.7027, which is much higher than the baseline's peak of 0.5515. Our model also demonstrates excellent precision and recall, and a lower false negative rate is crucial in the field of malicious URL detection, as we aim to minimize missing malicious URLs. The AUC of 0.9438 showcases the overall performance of our model on this unbalanced dataset.

We note that URLNet suffers from a high false positive rate, especially with smaller datasets, despite achieving high precision on larger datasets. Due to its reliance on the size and diversity of the training set, Grambeddings also encounters challenges. Our method shows consistent and reliable performance across diverse data distributions, indicating its ability to differentiate malicious and benign samples, and overcoming the challenges of imbalanced datasets better than other methods.

2) *Multiple classification*: To evaluate our method in the context of complex cyber threats, we conduct a multi-class

classification experiment, using a Kaggle 2 dataset [36] with four URL categories: benign (428,079), defacement (95,306), phishing (94,086), and malicious (23,645). Fig. 6 shows the results of our model and the baseline methods.

Fig.6 illustrates the performance of our method and the baseline methods across all four categories. Our method surpasses the baseline methods in each metric. The average ROC curve highlights our method's efficacy with a TPR of almost 90% at a low FPR of 0.001, surpassing other methods that achieve around 75%. Grambeddings struggled in recognizing negative samples from various categories, resulting in a 50% F1 score for defacement and phishing URLs and an overall accuracy of 83.91%. URLNet achieved an overall accuracy of 97.07%, falling short of our model's 98.57%.. These results demonstrate the robustness and effectiveness of our method in complex multi-class classification tasks, indicating its potential as a promising solution for malicious URL detection in cybersecurity.

### C. Cross-dataset testing

To assess the model's performance and generalization across different phishing datasets, and to identify potential weaknesses or biases within the model, we conducted a cross-dataset testing experiment. Specifically, we used the best-performing pre-trained model fine-tuned on the Grambeddings dataset and directly tested it on the Kaggle binary classification dataset. The results, as shown in Table VI, indicating that URLNet performs well, but Grambeddings has lower accuracy

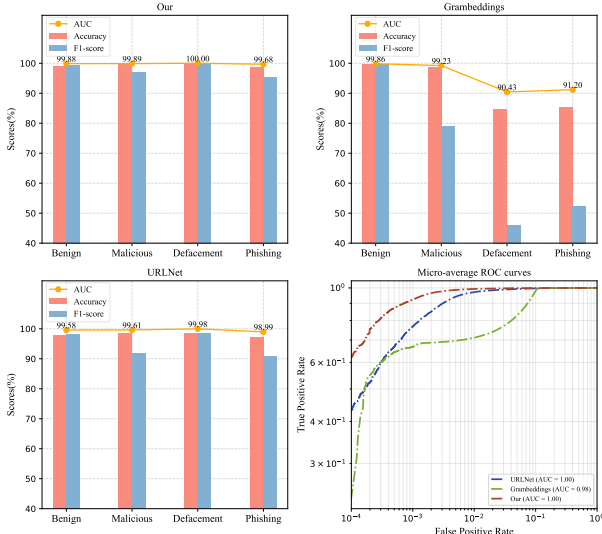


Fig. 6. Detection results of selected baseline methods and our proposed method on multiple classification dataset.

and AUC, with a high false positive rate (FPR) of 0.8667 despite having better recall.

In contrast, our model shows outstanding performance across all metrics, including high precision, recall, an F1 score close to 0.91, and a high AUC. Moreover, it excels in FPR, at 0.0185, surpassing both URLNet and Grambeddings. This is crucial in phishing URL detection models, as it emphasizes the need for low FPR to reduce false alarms in security services, ensuring benign URLs are not misclassified as phishing sites.

#### D. Evaluation against Adversarial Attacks

Cybercriminals employ adversarial attacks to bypass systems by exposing them to inaccurate, unrepresentative, or malicious data. We employed a Compound Attack technique as our threat model, which involves inserting an evasion character to a benign URL sample to create a real-world compatible malicious URL. This technique was first proposed by Maneriker *et al.* [10] and later applied and extended by Grambeddings [14].

The generation of adversarial samples entails the utilization of XLM-RoBERTa [37] for domain tagging in provided URLs. This process ensures a minimal tag count, involves the random insertion of hyphens in split parts, and includes the substitution of benign domains with malicious ones, resulting in the creation of an adversarial list.

To construct the AdvTest set, we merged 80K legitimate URLs and randomly sampled 40K malicious samples from the original validation data. Furthermore, we introduced 40K adversarial samples generated from benign URLs. This novel dataset presents a substantial challenge to the robustness of the model. Then we evaluate our and baseline models using this novel dataset.

As reported in the Figure 7 and TableVII, baseline methods experience notable performance degradation, whereas our model maintains stability with an AUC of 98.39%, surpassing

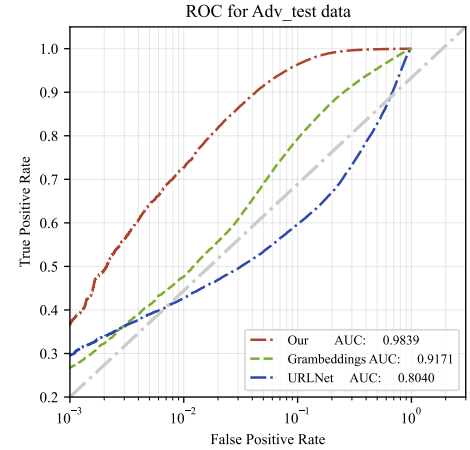


Fig. 7. Area under ROC curve under adversarial attack.

TABLE VII  
PERFORMANCE UNDER ADVERSARIAL ATTACK.

Method	ACC	P	R	F1	AUC
URLNet	0.7610	0.8745	0.5635	0.6854	0.8040
Gram	0.7018	0.6137	0.8564	0.8564	0.8564
Our	<b>0.9023</b>	<b>0.9738</b>	0.8104	<b>0.8846</b>	<b>0.9839</b>

URLNet by approximately 20 percentage points. At a fixed FPR of 0.01, our method achieves nearly 75% TPR, more than twice the TPR of baseline methods, both of which fall below 30%. These findings underscore the robustness of our method in real-world scenarios, effectively reducing false positives in security services even amid adversarial sample attacks.

#### E. Case Study

It is essential to evaluate a model in real-world phishing scenarios to understand its practical value. Therefore, we crawled the latest active phishing URLs reported and verified on Phish-Tank in November 2023 and conducted tests using models trained on the 30% Grambeddings dataset. Our model detects all malicious URLs with 100% accuracy, while Grambeddings misclassifies 7 URLs, achieving 76% accuracy, and URLNet misclassifies 4, resulting in 86% accuracy. Table VIII shows the misclassified URLs. URLNet tends to misclassify shorter URLs with fewer character features, while Grambeddings only achieves correct classification for URLs with explicitly malicious features. Grambeddings underperforms in real-world applications compared to its performance on the self-created dataset, showing a high error rate. N-grams break text into fixed-size chunks, leading to a wider and more uniform distribution of noise in the feature space, which makes it sensitive to minor fluctuations. Moreover, the Grambeddings method lacks specific feature refinement mechanisms, unlike URLNet, which uses max pooling within its CNN structure. Max pooling, though a simple operation, is effective in filtering out noise, allowing the model to focus on salient aspects of the data.

Our proposed approach uses multi-scale Learning and pyramid spatial attention mechanism, unlike the two baseline

TABLE VIII  
CROSS-DATASET PERFORMANCE GENERALIZATION

Malicious url	URLNet	Grambeddings	Our
<a href="https://bafybeibfyqcvrjmwlpiqkdyt2xr46cea7ldciglcbybfwtk7cieugcj3e.ipfs.infura-ipfs.io">https://bafybeibfyqcvrjmwlpiqkdyt2xr46cea7ldciglcbybfwtk7cieugcj3e.ipfs.infura-ipfs.io</a>	✓	✗	✓
<a href="http://798406.selcdn.ru/webmailprimeonline/index.html">http://798406.selcdn.ru/webmailprimeonline/index.html</a>	✓	✗	✓
<a href="https://79efc264-a0d7-4661-900b-a8bc1443be89.id.repl.co/biptoken.html">https://79efc264-a0d7-4661-900b-a8bc1443be89.id.repl.co/biptoken.html</a>	✓	✗	✓
<a href="http://ighjji.duckdns.org">http://ighjji.duckdns.org</a>	✗	✗	✓
<a href="https://www.minorpoint.lqoipum.top/">https://www.minorpoint.lqoipum.top/</a>	✓	✗	✓
<a href="https://colstrues.com/s/jsrj">https://colstrues.com/s/jsrj</a>	✗	✗	✓
<a href="https://innovativelogixhub.firebaseioapp.com/">https://innovativelogixhub.firebaseioapp.com/</a>	✓	✗	✓
<a href="https://sites.google.com/view/dejoelinoctskxo2bb">https://sites.google.com/view/dejoelinoctskxo2bb</a>	✗	✓	✓
<a href="https://gtly.to/-H0PPiKyq">https://gtly.to/-H0PPiKyq</a>	✗	✓	✓

**Note:** We use the symbols ✓ and ✗ to denote the correct and incorrect classification results, respectively.

methods. This enables learning feature importance and filtering noise across every dimension of the input representation space. As a result, our method shows improved accuracy in practical scenarios, especially in detecting challenging, hard-to-distinguish, or deceptive samples. This capability indicates a significant advancement in handling complex classification tasks in real-world applications.

## VI. DISCUSSION

We succinctly outline our methodology through several pivotal aspects:

- 1) **End-to-End Architecture:** Our method employs an end-to-end three-stage approach for inference, eliminating the need for expert manual feature engineering. Firstly, a subword tokenizer extracts the tokens from the URL. Secondly, transformer-based model generates two types of embedding vectors for the unknown URL and performs further processing. Finally, a classifier predicts the result, simplifying the feature engineering process and enhancing semantic understanding.
- 2) **Enhanced Learning Patterns through Hybrid Character and Word Embeddings:** Our model, utilizing character and word embeddings, achieves generalization to unknown URLs and overcomes constraints observed in prior dual-path networks (e.g., URLNet), such as insensitivity to changes in URL structures and semantics, and excessive reliance on training data scale. Our dual-channel pretrained model effectively addresses these issues.
- 3) **Stability and Robustness:** Our method overcomes the limitations of existing models in challenging scenarios. For example, Grambeddings struggles to accurately identify different types of malicious URLs in multi-class settings, while URLNet fails to detect any malicious samples in highly imbalanced datasets with small training sets, and both models show subpar performance under adversarial attacks and cross dataset test. In contrast, our approach exhibits significant improvements in all of these scenarios.
- 4) **Advanced Real-world Usability:** Our model exhibits exceptional performance on the latest reported URL dataset crawled from PhishTank, correctly identifying all malicious URLs. In contrast, baseline methods perform poorly in detecting real-world dynamic URLs, particu-

larly those with fewer features. These results demonstrate the significant practical value of our model.

- 5) **Streamlined Training and Efficient Deployment:** Our model achieves peak performance in only 5 training epochs—an exceptional improvement compared to the standard 20-30 epochs required by baseline methods. This remarkable efficiency is attributed to the efficient transfer of knowledge from the pretrained model to URL contexts and the integration of the lightweight multi-scale attention module. Furthermore, our model achieves optimal execution on a single GPU with over 20GB memory, delivering powerful performance while mitigating the need for high computational resources.

## VII. CONCLUSION

We have proposed a novel transformer-based and pyramid feature learning system called PyraTrans for malicious URL detection. Our method effectively leverages knowledge transfer from pretrained models to URL contexts, dynamically integrates character and subword-level features, and incorporates three closely integrated feature learning modules for URL feature extraction. The key contributions of our approach are: 1) enabling end-to-end learning from raw URL strings without manual preprocessing; 2) adopting an interactive subword and character-level feature learning network architecture for improved character-aware subword representations; 3) conducting effective multi-level and multi-scale URL feature learning based on our proposed lightweight feature learning modules, addressing inherent limitations of the Transformer in local feature extraction and spatial awareness. We conduct extensive experiments on various URL datasets, demonstrating that our method consistently outperforms existing state-of-the-art baseline methods and produces stable decisions across scenarios. Furthermore, our method exhibits superior generalization and robustness in cross-dataset detection and adversarial sample attacks, enhancing its reliability in practical applications. We also provide a case study with comparative analysis to demonstrate the practical value of our method.

## REFERENCES

- [1] I. consulting group, “Q3 2023 phishing and malware report,” Mar. 2023. [Online]. Available: <https://www.vadesscure.com/en/blog/q3-2023-phishing-malware-report>
- [2] J. C. Elaine Dzuba, “Introducing cloudflare’s 2023 phishing threats report,” Mar. 2023. [Online]. Available: <https://blog.cloudflare.com/2023-phishing-report/>

- [3] D. Sahoo, C. Liu, and S. C. Hoi, "Malicious url detection using machine learning: A survey," *arXiv preprint arXiv:1701.07179*, 2017.
- [4] T. Li, G. Kou, and Y. Peng, "Improving malicious urls detection via feature engineering: Linear and nonlinear space transformation methods," *Information Systems*, vol. 91, p. 101494, 2020.
- [5] M. S. I. Mamun, M. A. Rathore, A. H. Lashkari, N. Stakhanova, and A. A. Ghorbani, "Detecting malicious urls using lexical analysis," in *Network and System Security: 10th International Conference, NSS 2016, Taipei, Taiwan, September 28-30, 2016, Proceedings 10*. Springer, 2016, pp. 467–482.
- [6] R. Patgiri, A. Biswas, and S. Nayak, "deepbpf: Malicious url detection using learned bloom filter and evolutionary deep learning," *Computer Communications*, vol. 200, pp. 30–41, 2023.
- [7] T. Kim, N. Park, J. Hong, and S.-W. Kim, "Phishing url detection: A network-based approach robust to evasion," in *Proceedings of the 2022 ACM SIGSAC Conference on Computer and Communications Security*, 2022, pp. 1769–1782.
- [8] A. Blum, B. Wardman, T. Solorio, and G. Warner, "Lexical feature based phishing url detection using online learning," in *Proceedings of the 3rd ACM Workshop on Artificial Intelligence and Security*, 2010, pp. 54–60.
- [9] M. Korkmaz, E. Kocigit, O. K. Sahingoz, and B. Diri, "Phishing web page detection using n-gram features extracted from urls," in *2021 3rd International Congress on Human-Computer Interaction, Optimization and Robotic Applications (HORA)*. IEEE, 2021, pp. 1–6.
- [10] P. Maneriker, J. W. Stokes, E. G. Lazo, D. Carutasu, F. Tajaddodianfar, and A. Gururajan, "Urltran: Improving phishing url detection using transformers," in *MILCOM 2021-2021 IEEE Military Communications Conference (MILCOM)*. IEEE, 2021, pp. 197–204.
- [11] W. Chang, F. Du, and Y. Wang, "Research on malicious url detection technology based on bert model," in *2021 IEEE 9th International Conference on Information, Communication and Networks (ICICN)*. IEEE, 2021, pp. 340–345.
- [12] H. Le, Q. Pham, D. Sahoo, and S. C. Hoi, "Urlnet: Learning a url representation with deep learning for malicious url detection," *arXiv preprint arXiv:1802.03162*, 2018.
- [13] F. Tajaddodianfar, J. W. Stokes, and A. Gururajan, "Texception: a character/word-level deep learning model for phishing url detection," in *ICASSP 2020-2020 IEEE International Conference on Acoustics, Speech and Signal Processing (ICASSP)*. IEEE, 2020, pp. 2857–2861.
- [14] A. S. Bozkir, F. C. Dalgic, and M. Aydos, "Grambeddings: a new neural network for url based identification of phishing web pages through n-gram embeddings," *Computers & Security*, vol. 124, p. 102964, 2023.
- [15] J. Devlin, M.-W. Chang, K. Lee, and K. Toutanova, "Bert: Pre-training of deep bidirectional transformers for language understanding," *arXiv preprint arXiv:1810.04805*, 2018.
- [16] A. Radford, J. Wu, R. Child, D. Luan, D. Amodei, I. Sutskever *et al.*, "Language models are unsupervised multitask learners," *OpenAI blog*, vol. 1, no. 8, p. 9, 2019.
- [17] T. Brown, B. Mann, N. Ryder, M. Subbiah, J. D. Kaplan, P. Dhariwal, A. Neelakantan, P. Shyam, G. Sastry, A. Askell *et al.*, "Language models are few-shot learners," *Advances in neural information processing systems*, vol. 33, pp. 1877–1901, 2020.
- [18] Y. Huang, J. Qin, and W. Wen, "Phishing url detection via capsule-based neural network," in *2019 IEEE 13th International Conference on Anti-counterfeiting, Security, and Identification (ASID)*. IEEE, 2019, pp. 22–26.
- [19] H.-h. Wang, L. Yu, S.-w. Tian, Y.-f. Peng, and X.-j. Pei, "Bidirectional lstm malicious webpages detection algorithm based on convolutional neural network and independent recurrent neural network," *Applied Intelligence*, vol. 49, pp. 3016–3026, 2019.
- [20] C. Wang and Y. Chen, "Tcurl: Exploring hybrid transformer and convolutional neural network on phishing url detection," *Knowledge-Based Systems*, vol. 258, p. 109955, 2022.
- [21] M. Hussain, C. Cheng, R. Xu, and M. Afzal, "Cnn-fusion: An effective and lightweight phishing detection method based on multi-variant convnet," *Information Sciences*, vol. 631, pp. 328–345, 2023.
- [22] F. Zheng, Q. Yan, V. C. Leung, F. R. Yu, and Z. Ming, "Hdp-cnn: Highway deep pyramid convolution neural network combining word-level and character-level representations for phishing website detection," *Computers & Security*, vol. 114, p. 102584, 2022.
- [23] Y. Wang, W. Ma, H. Xu, Y. Liu, and P. Yin, "A lightweight multi-view learning approach for phishing attack detection using transformer with mixture of experts," *Applied Sciences*, vol. 13, no. 13, p. 7429, 2023.
- [24] P. Xu, "A transformer-based model to detect phishing urls," *arXiv preprint arXiv:2109.02138*, 2021.
- [25] Y. Wang, W. Zhu, H. Xu, Z. Qin, K. Ren, and W. Ma, "A large-scale pretrained deep model for phishing url detection," in *ICASSP 2023-2023 IEEE International Conference on Acoustics, Speech and Signal Processing (ICASSP)*. IEEE, 2023, pp. 1–5.
- [26] A. Singh, "Malicious and benign webpages dataset," *Data in brief*, vol. 32, p. 106304, 2020.
- [27] google, "google safe-browsing," Mar. 2023. [Online]. Available: <https://developers.google.com/safe-browsing>
- [28] W. Ma, Y. Cui, C. Si, T. Liu, S. Wang, and G. Hu, "Charbert: character-aware pre-trained language model," *arXiv preprint arXiv:2011.01513*, 2020.
- [29] Y. Deng, L. Wang, H. Jia, X. Tong, and F. Li, "A sequence-to-sequence deep learning architecture based on bidirectional gru for type recognition and time location of combined power quality disturbance," *IEEE Transactions on Industrial Informatics*, vol. 15, no. 8, pp. 4481–4493, 2019.
- [30] D. Hendrycks and K. Gimpel, "Gaussian error linear units (gelus)," *arXiv preprint arXiv:1606.08415*, 2016.
- [31] G. Jawahar, B. Sagot, and D. Seddah, "What does bert learn about the structure of language?" in *ACL 2019-57th Annual Meeting of the Association for Computational Linguistics*, 2019.
- [32] F. R. Li Ningjian, "Aspect-level sentiment analysis with fusion of multi-layer bert features," *Computer Science and Application*, vol. 10, p. 2147, 2020.
- [33] Y. Liu, X.-Y. Zhang, J.-W. Bian, L. Zhang, and M.-M. Cheng, "Samnet: Stereoscopically attentive multi-scale network for lightweight salient object detection," *IEEE Transactions on Image Processing*, vol. 30, pp. 3804–3814, 2021.
- [34] K. He, X. Zhang, S. Ren, and J. Sun, "Deep residual learning for image recognition," in *Proceedings of the IEEE conference on computer vision and pattern recognition*, 2016, pp. 770–778.
- [35] J. Guo, X. Ma, A. Sansom, M. McGuire, A. Kalaani, Q. Chen, S. Tang, Q. Yang, and S. Fu, "Spanet: Spatial pyramid attention network for enhanced image recognition," in *2020 IEEE International Conference on Multimedia and Expo (ICME)*. IEEE, 2020, pp. 1–6.
- [36] M. SIDDHARTH, "Malicious urls dataset," 2021. [Online]. Available: <https://www.kaggle.com/datasets/sid321axn/malicious-urls-dataset>
- [37] A. Conneau, K. Khandelwal, N. Goyal, V. Chaudhary, G. Wenzek, F. Guzmán, E. Grave, M. Ott, L. Zettlemoyer, and V. Stoyanov, "Unsupervised cross-lingual representation learning at scale," *arXiv preprint arXiv:1911.02116*, 2019.